




# Graphene reinforced aluminum nanocomposites: synthesis, characterization and properties

Binod Bihari Palei<sup>1</sup>, Tapan Dash<sup>1,2,\*</sup> , and Susanta Kumar Biswal<sup>1</sup>

<sup>1</sup>Centurion University of Technology and Management, Bhubaneswar, Odisha, India

<sup>2</sup>Tirupati Graphene and Mintech Research Centre, Bhubaneswar, Odisha, India

**Received:** 3 September 2021

**Accepted:** 22 February 2022

**Published online:**

14 March 2022

© The Author(s), under exclusive licence to Springer Science+Business Media, LLC, part of Springer Nature 2022

## ABSTRACT

Novel composites of Al–graphene (0.1–0.3 wt%) have been prepared by powder metallurgical processing. Powder composites were prepared by planetary ball milling route in toluene medium by 5 h of milling under inert atmosphere. Then, optimized high density compacted samples (prepared at 120 MPa) were sintered at 550 °C for 5 h. Various characterization of composites was done by using X-ray diffraction (XRD), X-ray photoelectron spectroscopy (XPS), field emission scanning electron microscopy, energy-dispersive spectroscopy (EDS), transmission electron microscope, high-resolution transmission electron microscope (HRTEM), selected area diffraction pattern (SAED), micro-Raman spectroscopy, electrical conductivity, and microhardness to obtain an Al–graphene composite with improved microhardness and electrical conductivity. Graphene was found in bi-layer form in the typical sample aluminum–graphene (0.2 wt%) composite. Purity of samples confirmed from EDS analysis showing only peaks of Al and C. XRD, XPS, HRTEM, and SAED studies establish the successful formation of Al and graphene composite. The typical aluminum–graphene (0.2 wt%) sample show significantly higher electrical conductivity ( $59.2 \times 10^6$  S/m) and microhardness ( $165 \pm 08$  VHN) values than that of pure aluminum, which shows electrical conductivity and microhardness values of  $38.0 \times 10^6$  S/m and  $65 \pm 05$  VHN, respectively. The results further advance electrical as well as structural, industrial applications of aluminum.

## Introduction

Nowadays, new materials with lightweight metal matrix composites have shown outstanding applications in the area of transport, construction, aerospace,

miniaturized microelectronic devices, thermoelectric materials, etc., due to a low-density structure, excellent thermal and electrical conductivity, and high mechanical strength, simultaneously [1–4]. Systematic observation with optimization of several critical parameters is required to produce specific desired

Handling Editor: M. Grant Norton.

Address correspondence to E-mail: tapanphy@gmail.com

outputs in the metal matrix composites. The quality of the final composite depends on some typical parameters such as weight percentage, volume fraction, size, shape, and orientation [5, 6]. The overall physical and chemical properties of composites depend on the dispersion nature of the reinforced phase, including uniformity, non-uniformity, isotropic or anisotropic distribution in the composites. Among these materials, the aluminum (Al)-matrix composites have been potentially focused on by the researchers owing to extraordinary properties such as extremely lightweight, flexibility, malleability, corrosion resistance, conductivity, and also its easy availability [7–12]. Among all the metals such as nickel, iron, magnesium, and chromium, it has the highest abundance in the earth's crust. It is commonly used in various commercial applications, including military applications such as helicopter instruments, flywheels, and the retainer rings used in high-speed motors, electronic/electrical equipment, automobile, and a large number of building materials [13–16]. But above applications are hardly observed in aluminum in its pure form. Therefore, excellent features and application areas can be better achieved when it is subjected to reinforcement agents, which yields successful composite with Al by improving uniform dispersion properly in the matrix. Generally, Al is used as a matrix phase in various material research and industrial fields for producing advanced and smart materials. Though aluminum metal and its alloys/composites are quite attractive, still its electrical and mechanical properties are limited in comparison to other advanced materials. It has been reported that various materials including SiC, C, Al<sub>2</sub>O<sub>3</sub>, SiO<sub>2</sub>, B, BN and B<sub>4</sub>C are added with the Al matrix to improve its properties [8, 17].

It is reported in the literature that reinforcements of CNTs (carbon nanotubes)/graphene have shown amazing scope to improve the properties of composites. This composite exhibits desired electrical, thermal, mechanical, and functional properties [9, 10]. Graphene has been considered to be better choice material in several research fields across the globe [10, 18–23]. Graphene is a single atomic layer of C arranged in a honeycomb lattice. The novel Al-graphene composite has great scope in material research [19, 20]. Aluminum-graphene composite has various potential applications because of exhibiting high strength, low density, and having excellent thermal and electrical conductivity. It can be used

automotive industry, piston combustion face for lowering engine emissions at elevated temperatures, transportation materials, preparing defense components, energy carrier material, wires and cables in motors for electric vehicles, aerospace, space, and satellite technologies, etc. [24–26]. This composite can be used for making piston rings, brake shoes, and various gears. In aerospace industries, brakes and landing gears are specially can be developed. They can be utilized in the making of antennas because of their good electrical conductivity. Because of having enhanced strength, lightweight bicycles and tennis rackets can be manufactured by this composite. These composites have a good surface area and high current density potential, which make them useful for energy storage purposes. These composites can be employed in anodes and coatings [27].

Some literature suggests graphene addition increases the electrical properties and microhardness when it is incorporated into aluminum to form aluminum-graphene composites, whereas it is also reported in the literature about the decrement values of such properties. Some typical literature reports related to our work are discussed here. Aluminum with 1 wt% of graphene exhibits microhardness increment up to 81 VHN in comparison to that of pure Al [19]. Literature reports [20] that Al with 0.1 wt% of graphene shows the hardness of 27.7 VHN only. This value increased to 28.5 VHN by increasing % of graphene up to 0.5 wt%. It has been observed that the hardness value increased when the sintering temperature increased from 550 to 650 °C [20]. The minimum hardness value of 27.7 VHN was obtained for the samples sintered at 550 °C (Al with 0.1 and 0.5 wt% graphene) while the maximum hardness value of 28.4 VHN was obtained for the samples sintered at 650 °C (Al with 0.1 wt% graphene) [20]. Sinter product (at 560 °C for 4 h) of pure aluminum and aluminum + 1 wt% graphene composite show hardness of ~ 35 VHN and ~ 75 VHN, respectively [28].

It was observed that the hardness of sintered (at 600 °C) pure Al and composite of Al/0.3 wt% of graphene nanoparticles were 76 and 85 VHN, respectively [29]. A higher hardness value of around 20 VHN was achieved for sintered aluminum-graphene composite (106 VHN) in comparison to the pure Al (81 VHN) [30]. In another work, the hardness of the pure aluminum was found to be  $64.0 \pm 2.0$  VHN, whereas by addition of the 0.7 wt% of graphene to Al matrix, the hardness

value raised to  $89.3 \pm 3.2$  VHN [31]. When the graphene % increases beyond 0.7 wt%, hardness value shows decreasing tendency. The hardness of pure aluminum, 0.1 wt% and 1.0 wt% graphene reinforcement composites show microhardness of 111, 98 and 97 VHN, respectively [32]. It was important to observe that when graphene content raised above 1% in aluminum matrix, the hardness value significantly reduced. The decrease in the hardness was due to difficulty in making uniform distribution of graphene reinforcement. The developed agglomeration tendency of graphene in the matrix resulted in decreasing mechanical properties of composites.

The electrical conductivity of Al/graphene (0.5 wt%) composites was achieved 8.9% more than that of pure Al [33]. At the same time, the electrical conductivity was reported to be 30.6% lesser than that of pure Al [34, 35]. This contradictory information observed in literature encouraged us to work on Al-graphene composite in view of improving properties.

In view of the above, it is worthwhile to mention that more research and systematic approaches are required to explore the properties of Al-graphene composites. In this study, composites of Al-graphene were prepared by 5 h of planetary ball milling of mixtures of Al and graphene (0.1–0.3 wt%) in toluene medium and under argon atmosphere. The following optimized parameters were adopted during the synthesis of composites: compaction of 120 MPa along with sintering at 550 °C. In this paper, an attempt has been made to prepare better quality aluminum-graphene composites without the formation of aluminum carbide phase. The composite properties were evaluated by using different techniques such as X-ray diffraction (XRD), field emission scanning electron microscopy (FESEM), X-ray photoelectron spectroscopy (XPS), energy-dispersive spectroscopy (EDS), transmission electron microscope (TEM), high-resolution transmission electron microscope (HRTEM), selected area diffraction pattern (SAED), micro-Raman spectroscopy, electrical conductivity, and microhardness.

## Experimental details

### Al-graphene composite preparation

The starting materials used for the preparation of composites were pure aluminum powder (purity 99%

and density 2.78 g/cc) and graphene (purity 99% and density 2.26 g/cc). At first, graphene was dispersed in 100 mL of ethanol using an ultrasonic bath (40 kHz) for 2 h, then the aluminum powder was added to it, and the mixture was thoroughly mixed. The weight percentage of graphene in the aluminum matrix was maintained at 0.1, 0.2 and 0.3 to obtain different Al-graphene composites. The mixed composites were subjected to ball milling, and the ball to powder ratio was maintained at 10:1. The ball milling was carried out for 5 h at 350 RPM under toluene atmosphere. After ball milling, different composites were dried in a vacuum oven for 24 h at 100 °C. Then, powders were taken for cold compaction at the pressure of 100–150 MPa to prepare samples of size around 20 mm diameter and 30 mm thickness. At 120 MPa, maximum compaction of composites was achieved. The compacted samples were subjected to sintering in a furnace at a temperature of 550 °C for 5 h under the argon atmosphere. Then, sintered samples were characterized and evaluated for the physical, electrical and microhardness properties by employing techniques.

### Determination of density of composites

At first, compaction of pure Al ball-milled sample was carried out a load of 100 MPa, 120 MPa and 150 MPa followed by sintering at 550 °C under argon atmosphere in a furnace for 5 h. From Table 1, it is observed that as compaction of load increase from 100 to 150 MPa, density was found to be increased. In our work, maximum densification was developed at a compaction load of 120 MPa because of improved packing between the powder particles. Following the above results, it was decided for compaction of Al-graphene (0.1–0.3 wt%) composites under the optimized load of 120 MPa followed by sintering of 550 °C for 5 h.

### Characterization of composites

PANalytical X'Pert Pro diffractometer equipped with Cu target was employed for recording X-ray diffraction patterns of various composites. Micro-Raman characterization of all samples was done by Renishaw inVia Reflex (UK) spectrometer. Morphological and elemental composition were carried out with the

**Table 1** Green and sintered density of pure aluminum and aluminum–graphene composites sintered at 550 °C for 5 h compacted at different applied loads

Sample ID	Compaction load (MPa)	Green density (g/cm <sup>3</sup> )	Sintered density (g/cm <sup>3</sup> )
Pure Al	100	2.424	2.499
	120	2.702	2.699
	150	2.678	2.698
Al–graphene (0.1 wt%)	120	2.666	2.689
Al–graphene (0.2 wt%)	120	2.612	2.655
Al–graphene (0.3 wt%)	120	2.605	2.644

help of field emission scanning electron microscope (FESEM) and energy-dispersive spectrometer (EDS) were used, which is made by ZEISS SUPRA 55 and Oxford, X-Max system attached with FESEM. In order to study the high-resolution morphological picture of samples, transmission electron microscope (TEM) was carried out (TECNAI G<sup>2</sup> (200 kV, FEI Netherland). At the time of TEM analysis, HRTEM pictures, SAED patterns and EDS characterizations were taken. 5 mL of ethanol was taken in a test tube. A very small quantity of sample was added to it. Then, the sample was sonicated for 30 min in an ultrasonic bath. Using a 10 µl pipette, take a small amount of liquid in the sonicated sample. Put a carbon-coated Cu grid with carbon face on top in a clean tissue paper, then add one drop of liquid with the sample to it and dry it using IR lamp. When it was completely dried, the sample was ready for testing in TEM. X-ray photoelectron spectroscopy (XPS) analysis was done for calculation of binding energy (B.E.) of different elements by using model S/N:1000:1, Privacy, Poland. The electrical conductivity of composites was measured by using Keithley 6221 Multimeter. With the help of tester-LECO with a load of 0.5 kg and 14 s dwell time, the microhardness of composites was determined by using Berkovich type diamond indenter. Density measurement of compacted pellets was determined ten times for each sample by following Archimedes principle by weighing the samples in the air as well as after dipping in 100 °C distilled water for 4 h. Further by using the four-probe method, electrical resistivity/conductivity (dc) was determined. Very fine *W* wire probes of 4 numbers were mounted on the pellet samples (circular in shape) at their central regions in a zone of 4 mm radius. Using the formula  $\rho = 2\pi s (V/I)$  [36, 37], resistivity/conductivity of samples was determined (where *V* is the voltage

between 2 inner probes and *I* is the current measured between 2 outer probes). Measurement parameters were as follows: current: 1 µA–100 mA, voltage: 1 nV–100 V. More than 10 readings per sample were carried out to calculate the arithmetic average values of resistivity/conductivity.

## Results and discussion

### XRD analysis

XRD patterns of pure aluminum and aluminum–graphene (0.1–0.3 wt%) composites (compactd at 120 MPa and sintered at 550 °C) are shown in Fig. 1. Pure aluminum shows only diffracted peaks of Al with the plane orientation of (111), (200) and (311). Al–graphene (0.1–0.3 wt%) composites show peak of Al and graphene. Graphene peak of C (002) is observed at around 2 theta of 26.5°, which is found to be similar to our earlier reported observation [38]. The typical Al–graphene (0.2 wt%) composite shows the relatively strong intense peak of graphene and Al. This result may be due to its good dispersion in Al matrix. Interestingly in this composite, it is also observed that FWHM of graphene peak is significantly higher than other Al–graphene composites. This outcome indicates reducing particle/grain size with proper exfoliation of different layers of graphene in the composite. XRD confirms the successful preparation of composites between aluminum and graphene.

From XRD spectra, the average crystallite size has been calculated for Al and C phases considering only their high intense peaks by applying Scherrer equation [39]:

$$\delta = 0.9\lambda/\beta \cos \theta \quad (1)$$

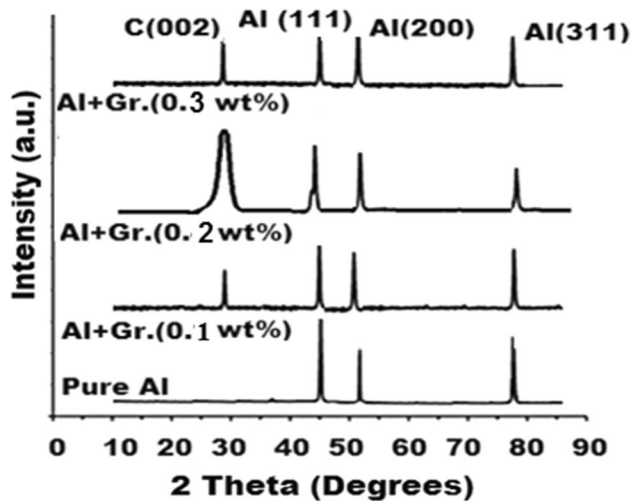


**Figure 1** XRD spectra of pure aluminum versus aluminum-graphene (0.1–0.3 wt%) composites.

where  $\lambda$  is the X-ray wavelength and  $\beta$  is the FWHM (full width at half maximum) in radian for the peak observed at  $2\theta$  diffracting angle. Al and C (graphene) show crystallite size in the range of  $\sim 80$ – $97$  nm and  $\sim 30$ – $62$  nm, respectively.

### Micro-Raman spectra

Micro-Raman spectra of sintered Al-graphene composites (compacted at 120 MPa and sintered at 550 °C) are shown in Fig. 2. Al is found absent in spectra because of its metallic nature. The Al-graphene (0.1–0.3 wt%) composites show 3 following peaks: lattice of graphite (G peak), first-order disorder in graphite lattice (D peak) and second-order disorder in graphite lattice (2D peak) [40, 41]. It is observed that Al with 0.2 wt% graphene exhibits downshifting of peak positions with relatively more broadening, which confirms about proper Bernal stacking of the graphene layers in the composite. This result also indicates a reduction in size of plane  $sp^2$  domains which is caused due to the optimized effect of ball milling. This result can be corroborated by the higher FWHM value observed for the graphene peak in its XRD study. A similar kind of observation is reported in the literature [40]. From micro-Raman spectra,  $I_G/I_{2D}$  (intensity ratio between G peak and 2D peak) was determined. The typical Al-graphene (0.2 wt%) composite infers  $I_G/I_{2D}$  ratio around 0.9, indicating bi-layer graphene present in the composite (Table 2).

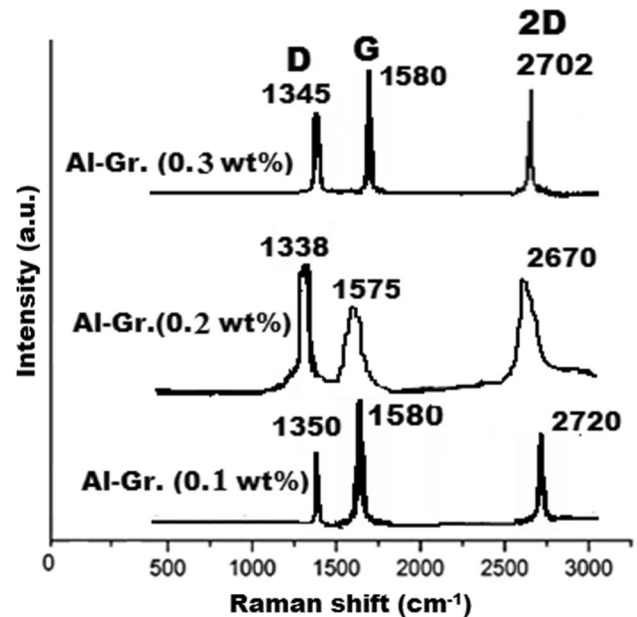


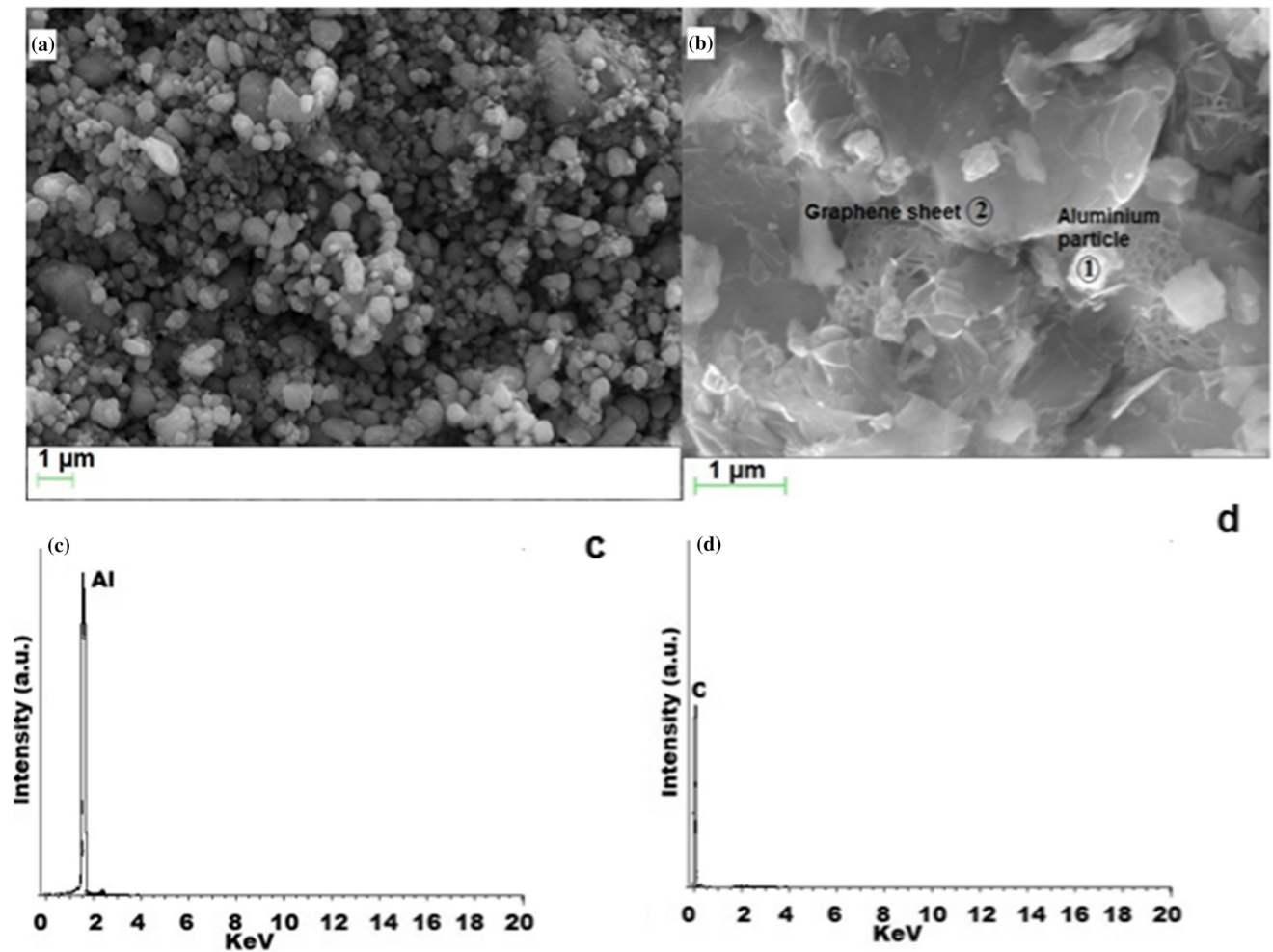
**Figure 2** Micro-Raman spectra of composites of aluminum-graphene (0.1–0.3 wt%).

### Microstructural investigation

FESEM analysis of pure Al and the typical Al-graphene (0.2 wt%) composite (prepared by compaction of 120 MPa and sintered at 550 °C) is presented in Fig. 3. FESEM result of ball-milled pure Al (Fig. 3a) shows high dense microstructural nature possible due to applying optimized compaction. The particle size was found to vary between 1 and 5  $\mu\text{m}$ . EDS analysis was carried out on FESEM image of typical Al-graphene (0.2 wt%) composite. EDS analysis of marked phase 1 in Fig. 3b presented in Fig. 3c show the peak of Al, whereas EDS carried out on marked phase 2 in Fig. 3b presented in Fig. 3d infers peak of C. In the EDS result, no impurity is traced. Graphene layers with transparency type microstructure were observed in the FESEM (Fig. 3b) microstructure of typical Al-graphene (0.2 wt%) composite. Graphene sheets were observed to be thin in structure. The composites show a high dense microstructure. No surface defect and porous behavior were observed from FESEM analysis. This shows the quality of composites prepared by the ball milling route followed by compaction and sintering. Such a type of microstructural improvement and level of dispersion of graphene phase in Al matrix is hardly found in the literature.

**Table 2** Raman shift and determination of  $I_G/I_{2D}$  values from micro-Raman spectra

Sample ID	D peak ( $\text{cm}^{-1}$ )	G peak ( $\text{cm}^{-1}$ )	2D peak ( $\text{cm}^{-1}$ )	$I_G/I_{2D}$
Al-0.1 wt% graphene	1350	1580	2720	1.3
Al-0.2 wt% graphene	1338	1575	2670	0.9
Al-0.3 wt% graphene	1345	1580	2702	1.2

**Figure 3** FESEM characterizations: **a** Pure Al, **b** Al–graphene (0.2 wt%) composite; EDS study on FESEM **b** of Al–graphene (0.2 wt%) composite: **c** EDS taken on marked phase 1; **d** EDS took on marked phase 2.

The TEM results of 0.1 wt% and 0.2 wt% of the graphene reinforced Al composites are shown in Fig. 4. Two types of phases, white and dark, were found to be developed in the composites. Composite with 0.1 wt% graphene (Fig. 4a) shows the non-homogeneous distribution of dark phases on white matrix, whereas the typical composite having 0.2 wt% graphene (Fig. 4b) almost shows the homogenous distribution of dark phases on white matrix. Well-defined-grained microstructures (Fig. 4b, c) were observed in composites with 0.2 wt% graphene.

0.3 wt% graphene reinforced Al composite shows non-homogeneous and agglomeration of phases in TEM image (Fig. 4d) similar to the microstructure observed for the 0.1 wt% graphene reinforced Al composite. Figure 4e shows HRTEM study taken on TEM (Fig. 4c) of Al–graphene (0.2 wt%) composite. Two kinds of lattice fringes inter-planar spacing of 0.333–0.334 nm and 0.223–0.224 nm are identified to be due to C (002) (graphene) and Al(111), respectively. SAED pattern of 0.2 wt% graphene with Al taken on its TEM image (Fig. 4c) is presented in

**Figure 4** TEM and HRTEM results of Al–graphene composites: **a** TEM of Al–graphene (0.1 wt%); **b** and **c** TEM of Al–graphene (0.2 wt%); **d** TEM of Al–graphene (0.3 wt%); **e** HRTEM of Al–graphene (0.2 wt%) taken on TEM **c**.

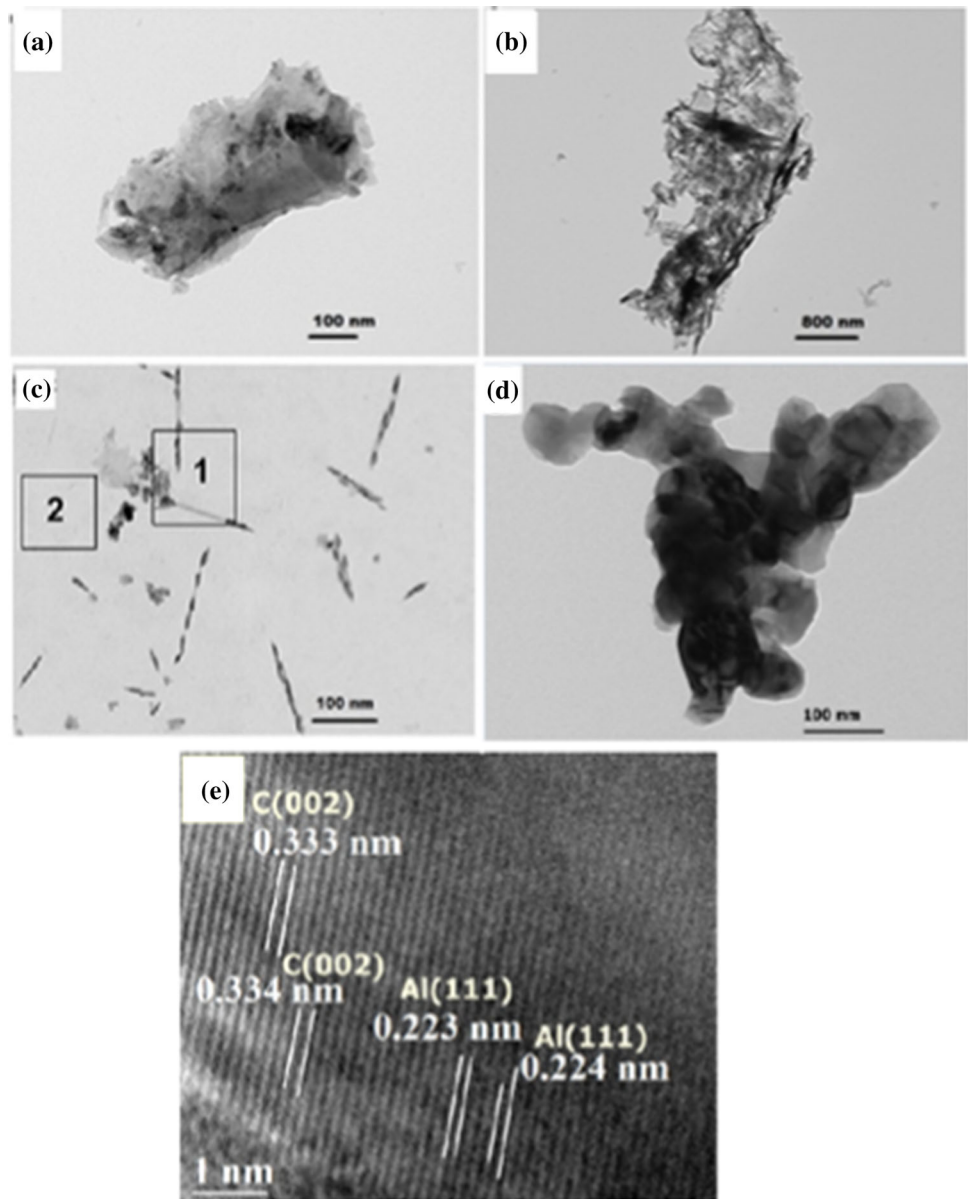
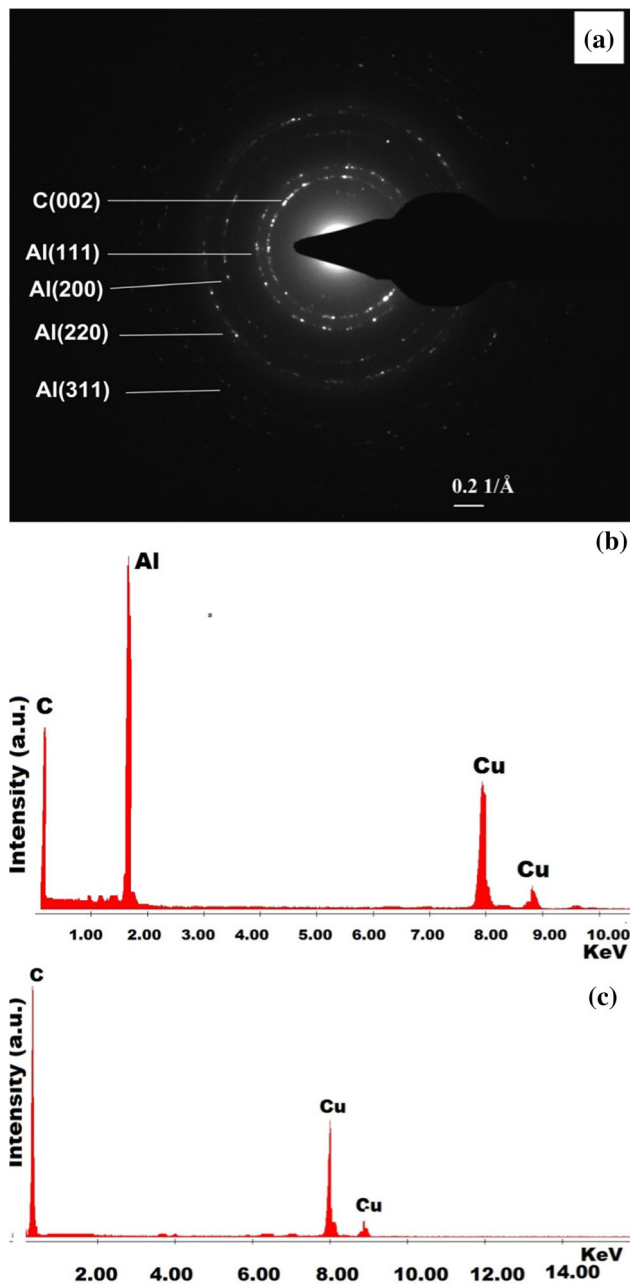


Fig. 5a. It shows diffracted spots with ring like patterns. SAED result indicates that even after ball milling followed by compaction and sintering the size of the unit cells of graphene and Al are not changed. The bright diffraction spots confirm the constitutes of composite as Al and C (graphene). The new Al (220) diffracted plane was observed SAED pattern, which was absent in its XRD result possibly due to its low intensity present in the pattern. HRTEM and SAED studies corroborated XRD and XPS characterization results for addressing the successful formation of Al and graphene composite without any presence of aluminum carbide. EDS analysis was carried out on TEM microstructure (Fig. 4c) for the identification of

white and dark grains. EDS analysis carried out on marked area 1 on Fig. 4c showed peaks of Al and C as shown in Fig. 5b. On the other hand, EDS analysis carried out on marked area 2 on Fig. 4c showed peaks of only C as shown in Fig. 5c.

Cu is shown in EDS because of using Cu coated carbon grid for TEM study. Al particles are found well dispersed and interacted in the larger sheet of graphene. TEM microstructure with sheet-like morphology and less contrast is indicating graphene in bi-layer/monolayer developed in the composite. On sheet of graphene, aluminum particles are almost uniformly distributed.



**Figure 5** a SAED result on TEM (Fig. 4c) of Al-graphene (0.2 wt%) composite; b and c EDS taken on TEM (Fig. 4c) of Al-graphene (0.2 wt) composite on marked phases 1 and 2, respectively.

### XPS study

Figure 6 and 7 shows XPS study in Al 2p and C 1s core levels of typical Al-graphene (0.2 wt%) composite compacted at 120 MPa and sintered at 550 °C. The analysis of the binding energies (B.E.s) shows Al atoms participation in Al–Al bonds and interaction of

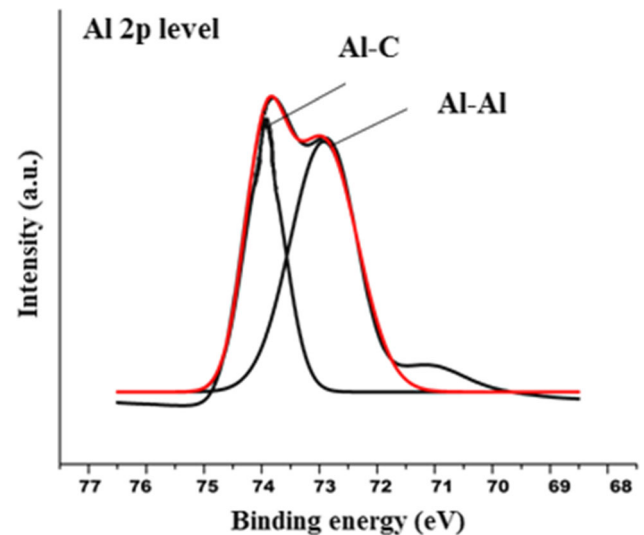


**Figure 6** De-convoluted Al 2p core level XPS spectra for typical Al-graphene (0.2 wt%) composite.

atoms for the formation of composite with C (graphene) by decreasing intensity corresponding to the lattice of Al. The peak identification was made by referring to the literature [42]. The Al 2p de-convoluted core level spectrum exhibits 2 peaks at 71.9 eV and 73.9 eV and corresponds to Al–Al (lattice bonding) and Al–C (bonding of the Al atoms with graphene), respectively. Here, C refers to graphene. The intensity of peak for Al–C is found higher than peak associated with Al–Al. It is maybe due to carbon being very sensitive to XPS analysis and layers of graphene are found to be almost coated/cover the grains of aluminum as seen in the FESEM analysis (Fig. 3b) of Al-graphene (0.2 wt%) composite. The specific surface area is very high in the case of graphene, i.e., 2630 m<sup>2</sup>/g, so 0.2 wt% can cover a large area in comparison to Al powder, increasing the intensity of Al–C in comparison to Al–Al. It may also be due to the strong bonding that exists between intercalated Al atoms and graphene interlayers. This provides Al matrix additional chemical forces (because of the strong Al–C interactions) and may strengthen the adhesion between Al and graphene, eventually having the scope to improve the mechanical property of the matrix. The assumption is reflected on the improvement of hardness of typical Al-graphene (0.2 wt%) composite in comparison to pure aluminum.

Similarly, C1s de-convoluted core level spectra exhibit peaks for bonding of the C atoms with Al(C–Al) and lattice bonding of C–C at B.E.s of 282.4 eV



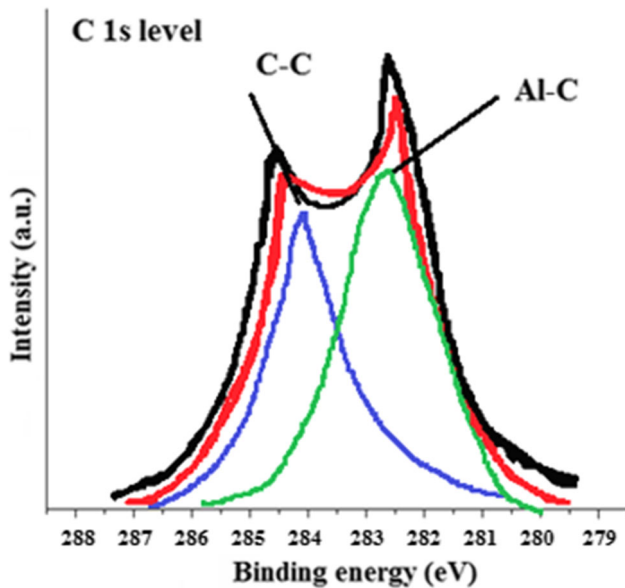


**Figure 7** De-convoluted C1s core level XPS spectra for typical Al-graphene (0.2 wt%) composite.

and 284.7 eV, respectively. The bonding between Al and C (graphene) confirms that Al atoms interacted in the graphene interlayer and make covalent bonding with the C atoms of graphene. This bonding will provide Al matrix with the additional molecular forces (due to Al–C interactions), which leads to enhancing the mechanical behavior of the composite.

### Determination of electrical conductivity and microhardness values

Electrical conductivity of sintered pure Al and Al-graphene composites (compacted at 120 MPa and sintered at 550 °C) were determined and presented in Table 3. Pure Al shows electrical conductivity of  $38 \times 10^6$  S/m. Among the samples, Al-graphene (0.2 wt%) composite shows significant improvement in electrical conductivity ( $59.2 \times 10^6$  S/m) in comparison to that of pure Al. Our observed electrical conductivity for Al with 0.2 wt% graphene was found to be higher than the reported value for Al with 0.5% graphene [35].

The microhardness of pure Al and Al-graphene composites (compacted at 120 MPa and sintered at 550 °C) were evaluated and presented in Table 3 and Fig. 8. Microhardness of pure Al was found  $65 \pm 08$  VHN. It is observed that increasing graphene % in the composites microhardness value increases. Al-

graphene (0.2 wt%) exhibits a higher hardness ( $165 \pm 08$  VHN) value than that of pure Al. The literature reports microhardness value for Al/0.6 wt% graphene nanoparticles is  $85 \pm 5$  VHN [29]. In other work, microhardness for Al-graphene (0.5 wt%) composite (compacted at 60 MPa and sintered at 650 °C) was determined around 28.4 VHN. Similarly, other researchers [10, 42] reported the hardness of graphene reinforced composites in the range of 89–122 VHN.

The literature reports three Al-*x*GNPs (*x* = 0, 0.5, 1.0 wt%) nanocomposites prepared by powder metallurgy route [43]. For the compaction of the powder sample, 500 MPa pressure was chosen. The sintering of composites was carried out for 6 h at 620 °C under an inert atmosphere (N<sub>2</sub>). The maximum hardness of  $57 \pm 4.2$  VHN was observed for Al-1.0 wt% GNPs composite. In the composite sample, a maximum density of  $2.695 \text{ g/cm}^3$  was observed for Al-0.5 wt% GNPs. Pure aluminum sintered sample shows a maximum sintered density of  $2.646 \text{ g cm}^{-3}$ . Impressive homogeneous distribution of graphene is found in aluminum matrix. But in our case, we prepared Al-graphene composites (0.1–0.3 wt%) at optimized compaction and sintering of 120 MPa and 550 °C for 5 h under the argon atmosphere, respectively. Our Al-graphene (0.2 wt%) composite shows more than 3× of hardness in comparison to the Al-1.0 GNPs. More analysis results of complex dielectric, complex electric modulus, and AC electrical conductivity were reported by the literature [44] for fabricated Al/(5% graphene (Gr)-PVA)/p-Si (metal-polymer-semiconductor) type structures for use in ultra-capacitor. An attempt had taken to develop a high dielectric material which leads to an increase in the capacitance, and it can store a higher charge of energy. But in our work, we have taken attempt to develop aluminum-graphene composites for various potential applications because of exhibiting high strength, low density and having excellent thermal and electrical conductivity. It can be used automotive industry, preparing defense components, energy carrier material, energy storage devices, aerospace, space, and satellite technologies, etc.

The observed hardness value in our work was found significantly higher than the reported value by other workers. In our work, microhardness and electrical conductivity of composite with 0.3 wt% graphene was found to show a lower value in comparison to that of 0.2% graphene. Relatively

**Table 3** Electrical conductivity and microhardness values determined for Al and Al–graphene composites

Sample ID	Electrical conductivity ( $\times 10^6$ S/m)	Microhardness in VHN
Al	38.0	$65 \pm 05$
Al–graphene (0.1 wt%)	44.43	$82 \pm 03$
Al–graphene (0.2 wt%)	59.1	$165 \pm 08$
Al–graphene (0.3 wt%)	54.6	$150 \pm 10$

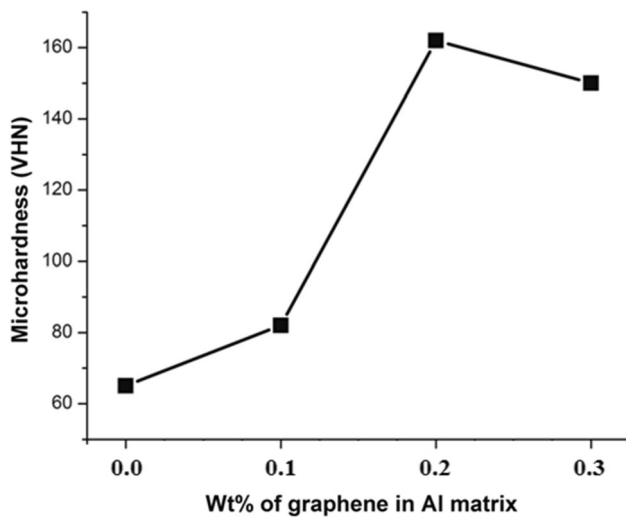


**Figure 8** Comparison of microhardness values of pure Al versus Al–graphene composites.

microhardness and electrical conductivity values of composite with 0.2% graphene are increased may be due to better packing developed between Al and graphene and almost homogenous distribution of graphene in Al matrix microstructure. Even after 0.2 wt% reinforcement of graphene, the density of composite was found to be  $2.655 \text{ g/cm}^3$ . The literature reports [45] that better final property of Al–graphene composite depends on the suitable amount of reinforcement of graphene with homogenous distribution, and strong interfacial bonding between graphene and Al matrix which is confirmed from our XPS study. In this work, the optimized composition is 0.2 wt% graphene reinforcement in aluminum matrix. Above the threshold, the properties will degrade beyond 0.2 wt% of graphene reinforcement, possibly because of the non-homogeneous or agglomeration formation of graphene in the Al matrix [45] as shown in the TEM image for 0.3 wt% graphene reinforced aluminum composite and can result in decreasing mechanical property of composite. With increasing graphene %, the number of particles present will increase and agglomerate at the grain boundary of aluminum. Refinement and

modification of grains lead to the finer size of grains. It increases more number of grain boundaries resulting in more resistance to electron motion which may also lead to a decrease in conductivity of the composite.

With increasing graphene %, more particles may be present in the grain boundary of aluminum which causes agglomeration and decreasing microhardness property of composite. Due to grain modification, finer becomes the grain size with increasing more number of grain boundaries; which strongly resist electron drifting and lead to decrease in electrical conductivity of the composite. From the results and discussion, it may be concluded that successful dispersion of graphene sheets in the matrix of Al and development of suitable bonding between Al and graphene under suitable compaction and sintering at optimized conditions can improve structural, electrical and mechanical properties of the composite.

## Conclusion

The work reports successful Al–graphene (0.1–0.3 wt%) composites preparation by 5 h of high energy ball milling followed by compaction and 5 h of sintering at  $550 \text{ }^\circ\text{C}$ . The density of pure Al was found to increase with increasing load from 100 to 150 MPa. The properties of pure Al and Al–graphene (0.1–0.3 wt%) composites prepared under the load of 120 MPa and sintered at  $550 \text{ }^\circ\text{C}$  were evaluated in this work. XRD along with XPS, FESEM, TEM, HRTEM and SAED studies confirm Al and graphene composite formation. Composites were free from oxidation and carbide forms of Al. This result was confirmed by EDS study. High transparency with very thin and reduced contrast of graphene phases was developed in the matrix of Al. The composite with 0.2 wt% graphene shows a mostly homogenous distribution of graphene in the composite. Different peaks of carbon such as D, G and 2D peaks were observed from Raman analysis. The microstructure of

graphene was found bi-layer. In contrast, pure Al shows hardness of  $65 \pm 05$  VHN; Al–graphene with 0.2 wt% shows hardness value of  $165 \pm 08$  VHN. The electrical conductivity of Al–graphene (0.2 wt%) was found better ( $59.2 \times 10^6$  S/m) than pure Al. Such microstructural, electrical conductivity and microhardness results confirm that Al–graphene composites were prepared under optimized ball milling, compaction and sintering conditions with improved properties.

## Declarations

**Conflict of interest** The authors declare that there have no conflict of interest.

## References

- [1] Tjong SC (2007) Novel nanoparticle-reinforced metal matrix composites with enhanced mechanical properties. *Adv Eng Mater* 9:639–652. <https://doi.org/10.1002/adem.200700106>
- [2] Surappa MK (2003) Aluminium matrix composites: challenges and opportunities. *Sādhanā* 28:319–334. <https://doi.org/10.1007/BF02717141>
- [3] Kumara M, Gupta RK, Pandey A (2019) Study on properties and selection of metal matrix and reinforcement material for composites. *AIP Conf Proc* 2148(030019):1–8
- [4] Lee HS, Jeon KY, Kim HY, Hong SH (2000) Fabrication process and thermal properties of SiC<sub>p</sub>/Al metal matrix composites for electronic packaging applications. *J Mater Sci* 35:6231–6236. <https://doi.org/10.1023/A:1026749831726>
- [5] He CL, Wang JM, Cai QK (2011) Effects of particle size and volume fraction on extrusion texture of SiC<sub>p</sub>/Al metal matrix composite. *Adv Mater Res* 194–196:1437–1441. <https://doi.org/10.4028/www.scientific.net/AMR.194-196.1437>
- [6] Hidalgo-Manrique P, Lei X, Xu R, Zhou M, Kinloch IA, Young RJ (2019) *J Mater Sci* 54:12236–12289. <https://doi.org/10.1007/s10853-019-03703-5>
- [7] Miracle DB (2005) Metal matrix composites from science to technological significance. *Compos Sci Technol* 65:2526–2540. <https://doi.org/10.1016/j.compscitech.2005.05.027>
- [8] Shabani MO, Mazahery A (2012) Optimization of process conditions in casting aluminum matrix composites via interconnection of artificial neurons and progressive solutions. *Ceram Int* 38:4541–4547. <https://doi.org/10.1016/j.ceramint.2012.02.031>
- [9] Konakov VG, Ovid'ko IA, Borisova NV, Solovyeva EN, Golubev SN, Kurapova O, Novik NN, Archakov IY (2014) Synthesis of the precursor for aluminum–graphene composite. *Rev Adv Mater Sci* 39:41–47
- [10] Wang J, Li Z, Fan G, Pan HH, Chen Z, Zhang D (2012) Reinforcement with graphene nanosheets in aluminum matrix composites. *Scr Mater* 66:594–597. <https://doi.org/10.1016/j.scriptamat.2012.01.012>
- [11] Kim BJ, Kim JP, Park JS (2014) Effects of Al interlayer coating and thermal treatment on electron emission characteristics of carbon nanotubes deposited by electrophoretic method. *Nanoscale Res Lett* 9:1–6. <https://doi.org/10.1186/1556-276X-9-236>
- [12] Li G, Xiong B (2017) Effects of graphene content on microstructures and tensile property of graphene-nanosheets/aluminum composites. *J Alloy Compd* 697:31–36. <https://doi.org/10.1016/j.jallcom.2016.12.147>
- [13] Miracle D (2005) Metal matrix composites—from science to technological significance. *Compos Sci Technol* 65:2526–2540. <https://doi.org/10.1016/j.compscitech.2005.05.027>
- [14] Rawal SP (2001) Metal-matrix composites for space applications. *JOM* 53:14–17. <https://doi.org/10.1007/s11837-001-0139-z>
- [15] Hidalgo-Manrique P, Yan SJ, Lin F, Hong QH, Kinloch IA, Chen X, Young RJ, Zhang XY, Dai SL (2017) Microstructure and mechanical behaviour of aluminium matrix composites reinforced with graphene oxide and carbon nanotubes. *J Mater Sci* 52:13466–13477. <https://doi.org/10.1007/s10853-017-1450-6>
- [16] Allison JE, Cole GS (1993) Metal-matrix composites in the automotive industry: opportunities and challenges. *JOM* 45:19–24. <https://doi.org/10.1007/BF03223361>
- [17] Niteeshkumar SJ, Keshavamurthy R, Haseebuddin MR, Koppad PG (2017) Mechanical properties of aluminum–graphene composite synthesized by powder metallurgy and hot extrusion. *Trans Indian Inst Met* 70:605–613. <https://doi.org/10.1007/s12666-017-1070-5>
- [18] Dash T, Rout TK, Palei BB, Bajpai S, Kundu S, Bhagat AN, Satpathy BK, Biswal SK, Rajput A, Sahu AK, Biswal SK (2020) Synthesis of  $\alpha$ -Al<sub>2</sub>O<sub>3</sub>–graphene composite: a novel product to provide multi-functionalities on steel strip surface. *SN Appl Sci* 2:1–9. <https://doi.org/10.1007/s42452-020-2672-9>
- [19] Sun C, Song M, Wang Z, He Y (2011) Effect of particle size on the microstructures and mechanical properties of SiC reinforced pure aluminum composite. *J Mater Eng Perform* 20:1606–1612. <https://doi.org/10.1007/s11665-010-9801-3>
- [20] Garg P, Gupta P, Kumar D, Parkash O (2016) Structural and mechanical properties of graphene reinforced aluminum matrix composites. *J Mater Environ Sci* 7:1461–1473

- [21] Chen F, Gupta N, Behera RK, Rohatgi PK (2018) Graphene-reinforced aluminum matrix composites: a review of synthesis methods and properties. *JOM* 70:837–845. <https://doi.org/10.1007/s11837-018-2810-7>
- [22] Liu N, Tang Q, Huang B, Yaping W (2022) Graphene synthesis: method, exfoliation mechanism and large-scale production. *Curr Comput-Aided Drug Des* 12:1–11. <https://doi.org/10.3390/cryst12010025>
- [23] Nieto A, Bisht A, Lahiri D, Zhang C, Agarwal A (2017) Graphene reinforced metal and ceramic matrix composites: a review. *Int Mater Rev* 62:241–302. <https://doi.org/10.1080/09506608.2016.1219481>
- [24] Palei BB, Dash T, Biswal SK (2020) A review on recent advances of aluminium/graphene nanocomposite. *PalArch's J Archaeol Egypt/Egyptol* 17:10119–10132. <https://archives.palarch.nl/index.php/jae/article/view/4049>
- [25] Pourmand NS, Asgharzadeh H (2019) Aluminum matrix composites reinforced with graphene: a review on production, microstructure, and properties. *Crit Rev Solid State Mater Sci* 45:289–337. <https://doi.org/10.1080/10408436.2019.1632792>
- [26] Cole G, Sherman A (1995) Lightweight materials for automotive applications. *Mater Charact* 35:3–9. [https://doi.org/10.1016/1044-5803\(95\)00063-1](https://doi.org/10.1016/1044-5803(95)00063-1)
- [27] Bakshi SR, Lahiri D, Agarwal A (2010) Carbon nanotube reinforced metal matrix composites—a review. *Int Mater Rev* 55:41–64. <https://doi.org/10.1179/095066009X12572530170543>
- [28] Kumar SJN, Keshavamurthy R, Haseebuddin MR, Koppad PG (2017) Mechanical properties of aluminium–graphene composite synthesized by powder metallurgy and hot extrusion. *Trans Indian Inst Met* 70:605–613. <https://doi.org/10.1007/s12666-017-1070-5>
- [29] Rashad M, Pan F, Tang A, Asif M (2014) Effect of graphene nanoplatelets addition on mechanical properties of pure aluminum using a semi-powder method. *Prog Nat Sci* 24:101–108. <https://doi.org/10.1016/j.pnsc.2014.03.012>
- [30] Azar MH, Sadri B, Nemati A, Angizi S, Shaeri MH, Minárik P, Veselý J, Djavanroodi F (2019) Investigating the microstructure and mechanical properties of aluminum-matrix reinforced-graphene nanosheet composites fabricated by mechanical milling and equal-channel angular pressing. *J Nanomater* 9:1–17. <https://doi.org/10.3390/nano9081070>
- [31] Du XM, Chen RQ, Liu FG (2017) Investigation of graphene nanosheets reinforced aluminum matrix composites. *Dig J Nanomater Biostruct* 12:37–45
- [32] Tabandeh-Khorshid M, Omrani E, Menezes PL, Rohatgi PK (2016) Tribological performance of self-lubricating aluminum matrix nanocomposites: role of graphene nanoplatelets. *Int J Eng Sci Technol* 19:463–469. <https://doi.org/10.1016/j.jestch.2015.09.005>
- [33] Rahimian M, Ehsani N, Parvin N, Baharvandi HR (2009) The effect of particle size, sintering temperature and sintering time on the properties of Al–Al<sub>2</sub>O<sub>3</sub> composites, made by powder metallurgy. *J Mater Process Technol* 14:5387–5393. <https://doi.org/10.1016/j.jmatprotec.2009.04.007>
- [34] Xu CL, Wei BQ, Ma RZ, Liang J, Ma XK, Wu DH (1999) Fabrication of aluminium–carbon nanotube composites and their electrical properties. *Carbon* 37:855–858. [https://doi.org/10.1016/S0008-6223\(98\)00285-1](https://doi.org/10.1016/S0008-6223(98)00285-1)
- [35] Chyada FA, Jabur AR, Alwan HA (2017) Effect addition of graphene on electrical conductivity and tensile strength for recycled electric power transmission wires. *Energy Procedia* 19:121–130. <https://doi.org/10.1016/j.egypro.2017.07.055>
- [36] Ferrari AC, Meyer JC, Scardaci V, Casiraghi C, Lazzeri M, Mauri F, Piscanec S, Jiang D, Novoselov KS, Roth S, Geim AK (2006) Raman spectrum of graphene and graphene layers. *Phys Rev Lett* 18(187401):1–4. <https://doi.org/10.1103/PhysRevLett.97.187401>
- [37] Ferrari AC (2007) Raman spectroscopy of graphene and graphite: disorder, electron–phonon coupling, doping and nonadiabatic effects. *Solid State Commun* 143:47–57. <https://doi.org/10.1016/j.ssc.2007.03.052>
- [38] Palei BB, Dash T, Biswal SK (2020) Reduced graphene oxide synthesis by dry planetary ball milling technique under hydrogen atmosphere. *IOP Conf Ser Mater Sci Eng* 872:1–6. <https://doi.org/10.1088/1757-899X/872/1/012158>
- [39] Patterson AL (1939) The Scherrer formula for X-ray particle size determination. *Phys Rev* 56:978–982. <https://doi.org/10.1103/PhysRev.56.978>
- [40] Dash P, Dash T, Rout TK, Sahu AK, Biswal SK, Mishra BK (2016) Preparation of graphene oxide by dry planetary ball milling process from natural graphite. *RSC Adv* 15:12657–12668. <https://doi.org/10.1039/C5RA26491J>
- [41] Kumar GR, Jayasankar K, Das SK, Dash T, Dash A, Jena BK, Mishra BK (2016) Shear-force-dominated dual-drive planetary ball milling for the scalable production of graphene and its electrocatalytic application with Pd nanostructures. *RSC Adv* 6:20067–20073. <https://doi.org/10.1039/C5RA24810H>
- [42] Czeppea T, Korznikova E, Ozga P, Wrobel M, Litynska-Dobrzynska L, Korznikova GF, Korznikov AW, Czaja P, Socha R (2014) Composition and microstructure of the Al–multilayer graphene composites achieved by the intensive deformation. *Acta Phys Pol B* 126:921–927. <https://doi.org/10.12693/APhysPolA.126.921>
- [43] Saboori A, Pavese M, Badini C, Fino P (2017) Microstructure and thermal conductivity of Al–graphene composites fabricated by powder metallurgy and hot rolling techniques.

- Acta Metall Sin (English Letters) 30:675–687. <https://doi.org/10.1007/s40195-017-0579-2>
- [44] Karadaş S, Yerişkin SA, Balbaş M, Kalandaraghbc YA (2021) Complex dielectric, complex electric modulus, and electrical conductivity in Al/(graphene-PVA)/p-Si (metal-polymer-semiconductor) structures. *J Phys Chem Solids* 148:109740. <https://doi.org/10.1016/j.jpcs.2020.109740>
- [45] Afifah MA, Omar MZ, Hashim H, Salleh MS, Mohamed IF (2021) Recent development in graphene-reinforced aluminium matrix composite: a review. *Rev Adv Mater Sci* 60:801–817. <https://doi.org/10.1515/rams-2021-0062>

**Publisher's Note** Springer Nature remains neutral with regard to jurisdictional claims in published maps and institutional affiliations.